Compounds Containing Copper−Sulfur Layers: Electronic Structure, Conductivity, and Stability

Grigori V. Vajenine and Roald Hoffmann*

Department of Chemistry, Cornell University, Ithaca, New York 14853-1301

Received August 9, 1995[⊗]

Compounds of the general formula $MCu_{2n}X_{n+1}$, where M is a monovalent metal and X is a chalcogen, exhibit relatively high conductivity and an interesting structural pattern of copper−chalcogen layers. The electronic structure of a series of copper−sulfur layers with the $Cu_{2n}S_{n+1}$ stoichiometry was studied using the extended Hückel method. Attention was focused on the unoccupied states at the top of the valence band. These states are Cu−S and Cu−Cu antibonding, which accounts for the observed contraction in the plane of the layers. The same states turn out to be strongly delocalized in the plane of the layers, with both copper and sulfur contribution; high mobility of holes in these states is responsible for the substantial conductivity observed in the corresponding materials. The idea of isodesmic reactions, borrowed from computational organic chemistry, was developed to address the relative stabilities of the copper−sulfur layers. We found the $Cu_2S_2^-$ layer to be less stable than the $Cu_4S_3^-$ layer, in accord with experiment.

Introduction

The subject of this paper is a remarkable, extensive series of ternary metal−copper−chalcogenides which contain stacked copper−chalcogen layers. Some representatives of this series have attracted attention because of high electrical conductivity[1] and an interesting structural relationship found in these materials.

The general formula for the compounds in this series is $MCu_{2n}X_{n+1}$ (M = Tl, K, Rb, Cs; X = S, Se, Te; n = 1, 2, 3); the examples that have been prepared and studied so far are shown in Table 1. The first member of the series—MCu_2X_2—adopts the $ThCr_2Si_2$ structure with Cu_2X_2 layers separated by M layers (see Figure 1, left). Each Cu_2X_2 layer is built up from edge-sharing CuX_4 tetrahedra. A similar structure is found in MCu_4X_3; edge-sharing CuX_4 tetrahedra now form thicker Cu_4X_3 layers, which are again isolated from each other

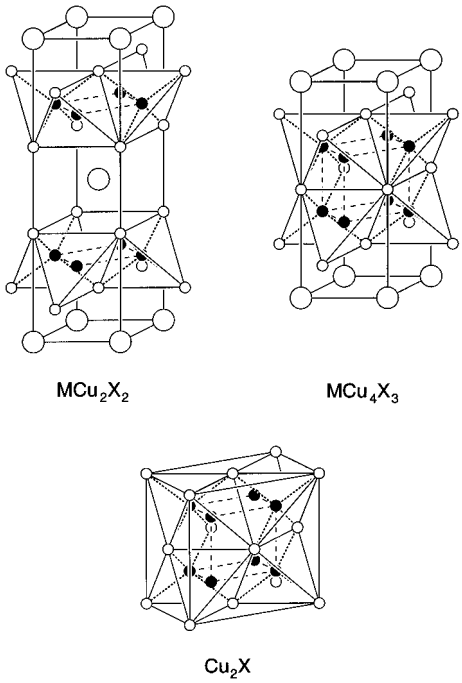

Figure 1. Conventional unit cells for MCu_2X_2, MCu_4X_3, and anti-fluorite-like Cu_2X. Large circles, small filled circles, and small unfilled circles represent M, Cu, and X, respectively. Solid lines indicate the boundaries of the unit cells and edges of CuX_4 tetrahedra, dotted lines represent some Cu−X bonds, and broken lines show shortest Cu−Cu contacts.

Table 1. Examples of Known Layered Monovalent Metal−Copper Chalcogenides

	X = S	X = Se	X = Te
n = 1	$TlCu_2S_2$[2−4]	$TlCu_2Se_2$[3,5−12]	$TlCu_2Te_2$[5,7]
n = 2	$TlCu_4S_3$[8,13]	$TlCu_4Se_3$[9,12,13]	
	KCu_4S_3[8,14−16]	KCu_4Se_3[8,13]	
	$RbCu_4S_3$[8,14,16]	$RbCu_4Se_3$[13]	
	$CsCu_4S_3$[13,16,17]	$CsCu_4Se_3$[13,18]	
n = 3	$TlCu_6S_4$[12,19,20]		

[⊗] Abstract published in *Advance ACS Abstracts,* December 15, 1995.

(1) Electrical conductivities have been reported for all compounds mentioned in Table 1 except for $TlCu_4S_3$ and (K, Rb, Cs)Cu_4Se_3. The range is from 40 to 43 000 Ω^{-1} cm^{-1} at room temperature; most of the values are on the order of 10^3−10^4 Ω^{-1} cm^{-1}. Please refer to Table 1 for references to individual compounds.
(2) Berger, R. *J. Less-Common Met.* **1989**, *147*, 141.
(3) Karlsson, L.; Keane, M. P.; Berger, R. *J. Less-Common Met.* **1990**, *166*, 353.
(4) Berger, R.; Dronskowski, R.; Norén, L. *J. Solid State Chem.* **1994**, *112*, 120.
(5) Tedenac, J.-C.; Brun, G.; Gardes, B.; Peytavin, S.; Maurin, M. *C. R. Seances Acad. Sci., Ser. C* **1976**, *283*, 529.
(6) Klepp, K.; Boller, H. *Monatsh. Chem.* **1978**, *109*, 1049.
(7) Brun, G.; Gardes, B.; Tedenac, J.-C.; Raymond, A.; Maurin, M. *Mater. Res. Bull.* **1979**, *14*, 743.
(8) Folmer, J. C. W.; Jellinek, F. *J. Less-Common Met.* **1980**, *76*, 153.
(9) Tedenac, J.-C.; Brun, G.; Maurin, M. *Rev. Chim. Miner.* **1981**, *18*, 69.
(10) Berger, R.; van Bruggen, C. F. *J. Less-Common Met.* **1984**, *99*, 113.
(11) Avilov, A. S.; Imamov, R. M.; Pinsker, Z. G. *Sov. Phys. Crystallogr. (Engl. Trans)* **1971**, *16*, 542.
(12) Berger, R. *Chem. Scr.* **1988**, *28*, 41.
(13) Klepp, K.; Boller, H.; Völlenkle, H. *Monatsh. Chem.* **1980**, *111*, 727.
(14) Rüdorff, W.; Schwarz, H. G.; Walter, M. *Z. Anorg. Allg. Chem.* **1952**, *269*, 141.
(15) Brown, D. B.; Zubieta, J. A.; Vella, P. A.; Wrobleski, J. T.; Watt, T.; Hatfield, W. E.; Day, P. *Inorg. Chem.* **1980**, *19*, 1945.
(16) Ghosh, B. P.; Chaudhury, M.; Nag, K. *J. Solid State Chem.* **1983**, *47*, 307.
(17) Burschka, C. *Z. Anorg. Allg. Chem.* **1980**, *463*, 65.
(18) Hartig, N. S.; Dorhout, P. K.; Miller, S. M. *J. Solid State Chem.* **1994**, *113*, 88.
(19) Berger, R. *Z. Kristallogr.* **1987**, *181*, 241.
(20) Berger, R.; Eriksson, L. *J. Less-Common Met.* **1990**, *161*, 165.

0020-1669/96/1335-0451$12.00/0

by layers of M. A building pattern emerges:[12,13,19,21,22] CuX_4 units share edges not only in the plane of the layers but, to some extent, also along the direction perpendicular to the plane of the layers (see Figure 1). As n in $MCu_{2n}X_{n+1}$ increases, the thickness of the $Cu_{2n}X_{n+1}$ layers increases, leading to the simple Cu_2X stoichiometry for very large values of n. This limiting structure corresponds to a copper chalcogenide with the antifluorite structure, with CuX_4 tetrahedra sharing edges in all three directions. The local geometry around Cu is different in $MCu_{2n}X_{n+1}$ from that in Cu_2X: the former set of compounds features CuX_4 tetrahedra that are slightly compressed in the plane of the layers, while the latter contains nearly ideal tetrahedra.

Another important feature of the compounds in this series is the presence of holes in the valence band.[23] Let us look at $TlCu_2X_2$ first. Assuming the formal oxidation state of +1 for thallium,[24] we obtain a −1 charge for a Cu_2X_2 unit. If both copper and the chalcogen were in closed shell oxidation states (+1 and −2, respectively), the charge on a Cu_2X_2 unit would be −2. Therefore, one hole per two coppers and two chalcogens is present in a Cu_2X_2 layer. A similar situation occurs in MCu_4X_3 and $TlCu_6S_4$ compounds: there is one hole per Cu_4X_3 (or Cu_6S_4) unit.

We restrict ourselves to the series with X = S in this study. As expected, the selenium and tellurium analogues have similar electronic structure and properties to those of the compounds in the sulfur series. Furthermore, we will focus on the isolated $Cu_{2n}S_{n+1}^-$ layers instead of three-dimensional $MCu_{2n}S_{n+1}$ solids; in the structures known the interlayer contacts are fairly long (the shortest S−S distances between the adjacent layers are 3.7−3.8 Å, out of the bonding range). The closed shell M^+ ions also do not perturb the electronic structure of the layers; we tested this point with some model calculations.

First, we will look at the electronic structure of two simple models—a tetrahedral CuS_4 fragment and bulk Cu_2S. Then the bonding nature of the states hosting the holes and its effect on the geometry of the layers will be addressed. We will also discuss the degree of delocalization of these states. Finally, the relative stability of the $Cu_{2n}S_{n+1}^-$ layers will be defined and discussed.

The extended Hückel method[25,26] was used in all calculations. Computational details, including atomic parameters, can be found in the Appendix.

From a CuS_4 Tetrahedron to Bulk Cu_2S

Before we can study the copper−sulfur layers, we need to become familiar with the electronic structure of the basic building block, a CuS_4 tetrahedron, and its three-dimensional analogue, bulk Cu_2S. Copper sulfide crystallizes in a slightly distorted antifluorite structure (mineral digenite), but its stoichiometry deviates from the ideal 2:1 ratio—the real material is copper-poor. The average Cu−S distance in $Cu_{1.79}S$ is 2.41 Å.[27] Since the CuS_4 fragment and bulk copper sulfide are used only as models to aid our understanding of the electronic structure of $MCu_{2n}S_{n+1}$, we choose all Cu−S distances in the two models to be the same (2.41 Å), the geometry around copper to be ideally tetrahedral, and the stoichiometry of the copper sulfide to be Cu_2S. We will refer to such a model of copper sulfide as model Cu_2S or simply Cu_2S.

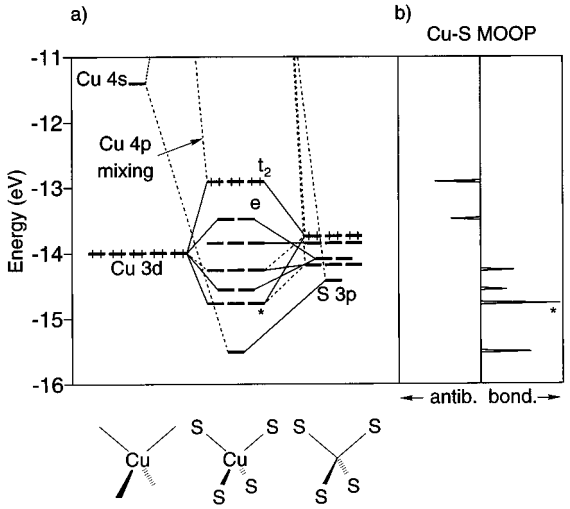

Figure 2. (a) Orbital interaction diagram for CuS_4^{7-}. The fragments are Cu^+ and S_4^{8-}. Solid lines indicate the strongest orbital mixing. Only electrons filling the HOMOs are shown. The asterisk marks the HOMO's bonding counterpart, discussed in the text. (b) Cu−S molecular orbital overlap population in CuS_4^{7-}.

The orbital interaction diagram for CuS_4^{7-} (the charge of −7 was chosen to preserve the closed shell configuration corresponding to Cu^+ and S^{2-}) and the results of the Cu−S molecular orbital overlap population (MOOP, a "solid-state-like" plot of the contribution of individual orbital to the specified overlap population) analysis are shown in Figure 2. A similar orbital pattern for CuS_4^{7-} was obtained in a related study on $BaCu_2S_2$.[28] The same study also addressed the bonding in the $Cu_2S_2^{2-}$ layer and found an electronic structure similar to that of the $Cu_2S_2^-$ layer discussed in the present work.

First, a typical "two below three" orbital splitting (Cu e below Cu t_2—HOMO) is observed, which is expected for a tetrahedral complex. However, the HOMO has a significant contribution from the 3p orbitals on sulfur (48%), because the H_{ii}s for Cu 3d and S 3p are accidentally identical. As expected, the HOMO is Cu−S antibonding. When a method that explicitly includes overlap between atomic orbitals is used, the interaction between atomic or fragment orbitals produces antibonding levels which are *more* antibonding than the corresponding bonding levels are bonding. However, the Cu−S overlap population plot for CuS_4^{7-} shows that the HOMO is *less* antibonding than its bonding counterpart is bonding. The reason for that is the mixing of Cu 4p into the HOMO with a phase that is Cu−S bonding, an example of a three-orbital interaction.[29]

The main electronic features of CuS_4^{7-} are preserved in bulk Cu_2S. Although most energy levels generate moderately wide bands, still the Cu t_2 states are generally slightly higher in energy than the Cu e states. The projection of the Cu t_2 contribution to the total density of states (DOS) peaks at a higher energy

(21) Makovicky, E.; Johan, Z.; Karup-Møller, S. *Neues Jahrb. Mineral. Abh.* **1980**, *138*, 122.
(22) Zheng, C.; Hoffmann, R. *J. Am. Chem. Soc.* **1986**, *108*, 3078.
(23) The presence of holes in the valence band in these ternary metal−copper−chalcogenides was demonstrated experimentally by Brun *et al.* (ref 7), Folmer and Jellinek (ref. 8), Berger and van Bruggen (ref 10), and Berger (ref 2) on the basis of the results of Hall effect measurements.
(24) For Tl there is in principle an alternative, a +3 oxidation state. A referee suggested that assigning a +3 oxidation state to some Tl centers would reduce the number of Cu^{2+} ions in $TlCu_2S_2$, thus placing some holes on thallium.
(25) Hoffmann, R. *J. Chem. Phys.* **1963**, *39*, 1397.
(26) Landrum, G. Yet Another Extended Hückel Molecular Orbital Package (YAeHMOP). Cornell University, 1995. YAeHMOP is available on the World Wide Web at: http://overlap.chem.cornell.edu:8080/yaehmop.html.
(27) Lide, D. R., Ed. *CRC Handbook of Chemistry and Physics*, 75th ed.; CRC: Boca Raton, FL, 1994; Section 4-142.
(28) Ouammou, A.; Mouallem-Bahout, M.; Peña, O.; Halet, J.-F.; Saillard, J.-Y.; Carel, C. *J. Solid State Chem.* **1995**, *117*, 73.
(29) Albright, T. A.; Burdett, J. K.; Whangbo, M.-H. *Orbital Interactions in Chemistry*; Wiley: New York, 1985.

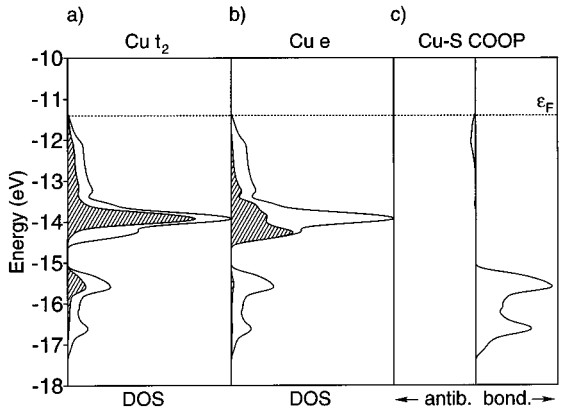

Figure 3. (a) Total DOS (solid line) and projection of Cu t_2 (lined) for Cu_2S. (b) Total DOS and projection of Cu e for Cu_2S. (c) Cu−S COOP plot for Cu_2S.

than does the projection of the Cu e contribution; also the Cu t_2 states contribute more than the Cu e states contribute to the top of the valence band (see Figure 3). The Cu−S crystal orbital overlap population[30] (COOP) plot indicates that the upper band ("Cu 3d band") is very weakly Cu−S antibonding, whereas the lower band ("S 3p band") is Cu−S bonding. Again, as in CuS_4^{7-}, antibonding is weaker than bonding due to even more substantial mixing of Cu 4p states into the Cu 3d band.

Distortions in $Cu_{2n}S_{n+1}$ Layers

We mentioned earlier that although the copper−sulfur layers contain CuS_4 tetrahedra, these tetrahedra are distorted. First, we need to define the distortions. It is useful to focus on another view of this structure, in terms of square nets of copper and sulfur which make it up. Such a representation is shown in **1**, using Cu_2S_2 as an example.

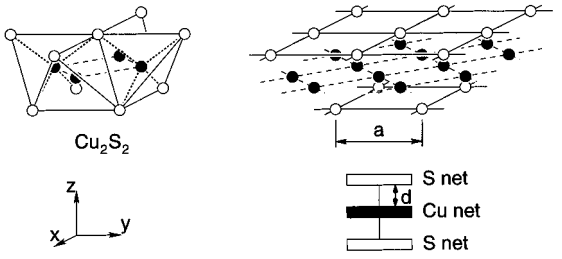

1

Note that the separation between the nets (*d*) and the nearest neighbor S−S separation within a sulfur net (*a*) completely describe the geometry of a Cu_2S_2 layer. The other layers in the series (Cu_4S_3, Cu_6S_4, and, ultimately, Cu_2S) also can be described by a similar set of parameters, although several copper-net-to-sulfur-net distances need to be used. The first parameter, *a*, is also the lattice parameter in the *xy* plane for the corresponding tetragonal unit cell; these values have been measured reliably for all compounds in the series. The separation between copper and sulfur nets, *d*, is also known accurately for most of the ternary metal−copper−chalcogenides.

The following values of *a* are observed in the $TlCu_{2n}S_{n+1}$ series (see Table 2): 3.94 Å in the model Cu_2S, 3.95 Å in $TlCu_6S_4$, 3.90 Å in $TlCu_4S_3$, and 3.78 Å in $TlCu_2S_2$. A trend is apparent: a contraction in the *xy* plane takes place on moving from Cu_2S to $TlCu_2S_2$. This has been previously related to the increasing effect on one hole per $Cu_{2n}S_{n+1}$ unit: as *n* decreases,

(30) Hoffmann, R. *Solids and Surfaces: A Chemists's View of Bonding in Extended Structures*; VCH: New York, 1988.

Table 2. S−S Distances in Sulfur Nets (*a*) and Copper-Net-to-Sulfur-Net Separations (*d*) in Ternary Monovalent Metal−Copper−Sulfides[a]

	a, Å	*d*, Å
$TlCu_2S_2$	3.78	1.34
$TlCu_4S_3$	3.90	1.50 (d_{inner}), 1.25 (d_{outer})
KCu_4S_3	3.90	1.49 (d_{inner}), 1.24 (d_{outer})
$RbCu_4S_3$	3.92	
$CsCu_4S_3$	3.97	1.46 (d_{inner}), 1.19 (d_{outer})
$TlCu_6S_4$	3.95	1.34 (innermost), 1.58, 1.18 (outermost)
model Cu_2S	3.94	1.39

[a] See text structures **1** and **2** for the definitions of *a*, *d*, d_{inner}, and d_{outer}. Three different values of *d* are needed to describe $TlCu_6S_4$.

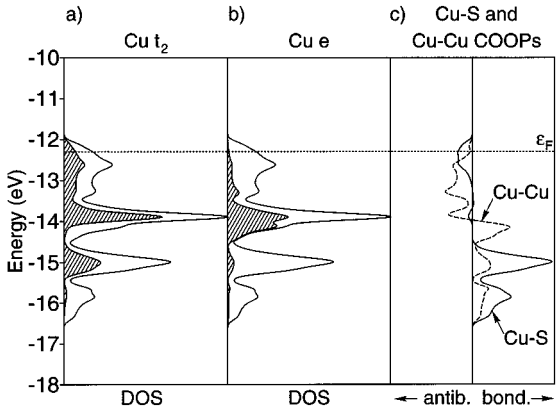

Figure 4. (a) Total DOS (solid line) and projection of Cu t_2 (lined) for idealized $Cu_2S_2^-$. (b) Total DOS and projection of Cu e for $Cu_2S_2^-$. (c) Cu−S and Cu−Cu COOP plots for $Cu_2S_2^-$. The Cu−Cu COOP is magnified 3-fold with respect to the Cu−S COOP.

the copper−sulfur layer becomes thinner.[2,12] We will now look at the bonding nature of the energy levels where these holes are located.

First, the band structure for a model Cu_2S_2 layer will be discussed, with all CuS_4 tetrahedra in the layer taken to be ideal and all Cu−S distances equal to 2.41 Å. This geometry corresponds to $a = 3.94$ Å and $d = 1.39$ Å. The local geometry around copper in the model Cu_2S_2 is the same as it is in bulk Cu_2S; therefore, a similar electronic structure is expected. The computed density of states, copper t_2 and e contributions to the DOS, and Cu−S and Cu−Cu COOP plots are shown in Figure 4.

The most important difference between the model $Cu_2S_2^-$ layer and bulk Cu_2S is that in the former the Fermi level cuts through the top of the valence band. The dispersion of the bands of the three-dimensional material is generally a little greater. In other respects the two systems have similar electronic structures.

The states immediately above the Fermi level in the model $Cu_2S_2^-$ are almost equally distributed between copper and sulfur. As in CuS_4 and Cu_2S, these states are only weakly Cu−S antibonding due to Cu 4p mixing.[31] They are also weakly Cu−Cu antibonding (the Cu−Cu distance is relatively long—2.79 Å).

Depopulation of antibonding states in model $Cu_2S_2^-$ relative to Cu_2S suggests stronger bonds, therefore shortening of Cu−S and Cu−Cu distances. However, the coordination of sulfur differs drastically in the two structures, so direct comparison of Cu−S bonds is not appropriate in this case. A more accurate way of probing this distortion is to study the compression of

(31) As pointed out by a referee, the states at the top of the Cu−S valence band are not always Cu−S antibonding in copper sulfides, $TlCu_3S_2$ being an example (see ref 4).

the model $Cu_2S_2^-$ layer in the *xy* plane, thus decreasing *a* and keeping the copper-net-to-sulfur-net separation *d* constant. The energy of such a compressed layer ($a = 3.78$ Å) was computed to be 0.318 eV per unit cell lower than the energy of the model $Cu_2S_2^-$ layer ($a = 3.94$ Å). One has to accept this result with caution, because the extended Hückel method is known to underestimate bond lengths.

To see more clearly the influence of the holes, a comparison to a material without holes that is more structurally similar to $Cu_2S_2^-$ than Cu_2S has to be made. A $Cu_2S_2^{2-}$ layer with one more electron per unit cell than $Cu_2S_2^-$ (and therefore no holes in the valence band) is the perfect candidate. We compute the energy of compressed $Cu_2S_2^{2-}$ ($a = 3.78$ Å) to be only 0.094 eV per unit cell lower than the energy of model $Cu_2S_2^{2-}$ ($a = 3.94$ Å). This implies that the presence of holes by itself creates a substantial driving force toward compression in the *xy* plane.

The construction of the model $Cu_2S_2^{2-}$ layer is not unrealistic; there exist compounds, such as $BaCu_2S_2$, containing this formally doubly charged layer. Interestingly, the experimentally found geometry of this layer[32] ($a = 3.91$ Å, $d = 1.42$ Å, Cu−S distance of 2.41 Å) is very similar to what we use as the model Cu_2S_2 geometry based on the copper sulfide structure. The fact that the value of *a* in $TlCu_2S_2$ is less than that in $BaCu_2S_2$ also confirms the effect of holes on the contraction of the Cu_2S_2 layer.

A similar picture holds for the other compounds in the $MCu_{2n}S_{n+1}$ series: one hole per $Cu_{2n}S_{n+1}^-$ unit is present in the valence band and the states immediately above the Fermi level are computed to be both Cu−S and Cu−Cu antibonding. However, as *n* increases, so does the size of the $Cu_{2n}S_{n+1}^-$ unit, and the contracting effect of the hole decreases. This is in accord with the experimentally observed trend: *a* increases with *n*. The contraction is virtually gone by the time *n* reaches 3 ($TlCu_6S_4$).

The other distortion from the model $Cu_{2n}S_{n+1}$ structure is the relative motion of Cu and S nets along the *z* axis (perpendicular to the plane of the layer). This motion changes the copper-net-to-sulfur-net separations *d*. Now we will look at the variations in the values of *d* in MCu_4S_3 (M = Tl, K, Cs). Two different *d* parameters, d_{inner} and d_{outer}, are needed to describe the structure of the Cu_4S_3 layer:

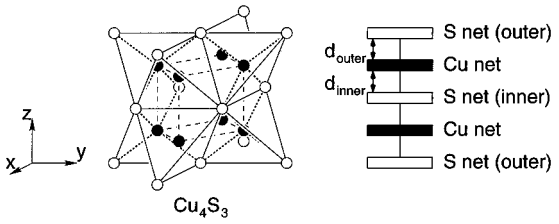

2

The values of d_{inner} and d_{outer} do not vary much in this group of compounds (see Table 2); d_{inner} is 150, 1.46, and 1.49 Å and d_{outer} is 1.25, 1.19, and 1.24 Å in $TlCu_4S_3$, $CsCu_4S_3$, and KCu_4S_3, respectively. The lattice parameter in the *xy* plane, *a*, is more sensitive to the size of the M^+ cation; it takes on values of 3.90 ($TlCu_4S_3$ and KCu_4S_3), 3.92 ($RbCu_4S_3$), and 3.97 Å ($CsCu_4S_3$).

To rationalize the fact that $d_{inner} > d_{outer}$, we carried out a calculation on the model $Cu_4S_3^-$ layer with d_{inner} and d_{outer} being held the same (1.39 Å) and *a* fixed at 3.90 Å. The computed Cu−S overlap population values were 0.235 for the bonds between a copper net and the inner sulfur net, and 0.278 for the bonds between a copper net and the nearest outer sulfur net. Thus the latter bonds are stronger than the former, which agrees with d_{inner} being greater than d_{outer} (using the "a stronger bond is a shorter bond" rationale). But why are the Cu−S (outer) bonds stronger than the Cu−S (inner) bonds to begin with? The outer S atoms are bonded to only four neighboring Cu atoms in a square-pyramidal fashion, whereas the inner S atoms have eight Cu neighbors forming a cube. All Cu−S bonds are strongly covalent, and there are simply insufficient electrons to form eight Cu−S (inner) bonds which are as strong as the four Cu−S bonds around the outer S atoms.

The copper-net-to-sulfur-net separation in $TlCu_2S_2$ is 1.34 Å, which is also less than the value of 1.39 Å in the model Cu_2S. The distance from the outermost sulfur net to the closest copper net in $TlCu_6S_4$ is only 1.18 Å, the smallest of the three values of *d*. This is analogous to d_{outer} in MCu_4S_3 being the shortest copper-net-to-sulfur-net separation.

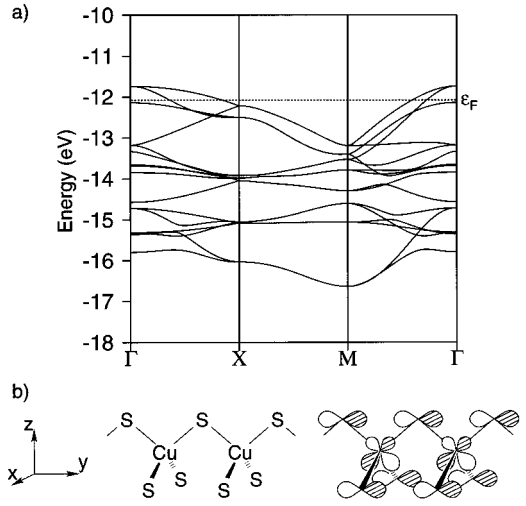

Figure 5. (a) Band structure for $Cu_2S_2^-$ computed with a $a = 3.78$ Å. (b) One of the two crystal orbitals immediately above the Fermi level at the Γ point.

$Cu_2S_2^-$: Electrical Conductivity

In the previous section we discussed the bonding nature of the states around the Fermi level in the $Cu_2S_2^-$ layer; now we will address the effect of holes in these states on electrical conductivity. All results presented in this section were computed with $a = 3.78$ Å and $d = 1.39$ Å (a $Cu_2S_2^-$ layer compressed in the *xy* plane).

The total DOS, as well as projections of Cu t_2 and Cu e states (not shown here), are similar to those shown in Figure 4 for model $Cu_2S_2^-$ ($a = 3.94$ Å and $d = 1.39$ Å). The states immediately above the Fermi level are 44% on Cu and 56% on S; the major part of the copper contribution comes from Cu t_2 states. Both S p_x, p_y (in the plane of the layer) and S p_z (perpendicular to the plane of the layer) contribute to the states in question. The band structure for the compressed layer is shown in Figure 5.

There are two bands that host holes; most of the holes are concentrated around the center of the Brillouin zone. These bands are made purely of Cu d_{xz}, d_{yz} and S p_x, p_y (with a moderate admixture of Cu p_x, p_y) at the Γ point. One of the two representative hole crystal orbitals is drawn in Figure 5

(32) See ref 28. A referee brought to our attention other important studies on tetragonal $BaCu_2S_2$: Savel'eva, M. V.; Trushnikova, L. N.; Kamarzin, A. A.; Alekseev, V. I.; Baidina, I. A.; Borisov, S. V.; Gromilov, S. A.; Blinov, A. G. *Izv. Akad. Nauk SSSR, Neorg. Mater.* **1990**, *26*, 2653. Saeki, M.; Onoda, M.; Nozaki, H. *Mater. Res. Bull.* **1988**, *23*, 603. Onoda, M.; Saeki, M. *Mater. Res. Bull.* **1989**, *24*, 1337. Orthorhombic $BaCu_2S_2$ and $BaCu_2Se_2$ also have been reported: Iglesias, J. E.; Pachali, K. E.; Steinfink, H. *Mater. Res. Bull.* **1972**, *7*, 1247. Iglesias, J. E.; Pachali, K. E.; Steinfink, H. *J. Solid State Chem.* **1974**, *9*, 6.

(this is the orbital at Γ, at −11.7 eV). Each of the two bands develops some S p_z and Cu $d_{x^2-y^2}$ (as well as Cu p_z) character in other points of the Brillouin zone. The coordinate system used is such that $d_{x^2-y^2}$, d_{xz}, and d_{yz} constitute the Cu t_2 block.

Copper d orbitals and sulfur p orbitals in these bands are out of phase with each other, consistent with their Cu−S antibonding nature discussed previously. Note that all three bands are substantially delocalized in the plane of the layer, and all Cu d−S p overlaps involved are large, thus making high mobility of holes in these bands possible.

X-ray photoelectron spectroscopy has been used[3,8] to determine the most likely oxidation states of copper and sulfur in compounds containing singly charged layers. The goal was to elucidate the location of holes. Formally, one could assume that the holes are located either entirely on copper (e.g. $(Cu^{1.5+})_2(S^{2-})_2$), entirely on sulfur (e.g. $(Cu^{+})_2(S^{1.5-})_2$), or partially on both. The results of these experimental studies conducted on $TlCu_2S_2$, $TlCu_4S_3$, and KCu_4S_3 indicate that the oxidation state of copper is better described as +1, thus placing the holes in sulfur 3p levels.

Our calculations imply, as mentioned above, that the holes are approximately equally distributed among copper and sulfur atoms. However, this distribution is sensitive to the choice of the atomic parameters. The H_{ii} for the sulfur 3p orbitals was optimized to give a reasonable charge distribution in bulk copper sulfide: a small negative charge on sulfur (−0.20) and a small positive charge on copper (+0.10), in accord with the relative electronegativities. When another parameter set was used (with S 3p H_{ii} of −11.0 eV), the holes in $Cu_2S_2^-$ shifted mainly to sulfur, while retaining some (19%) copper character. The latter parameter set also produced a counterintuitive charge distribution in bulk Cu_2S (+0.50 on sulfur and −0.25 on copper).[33]

Either set of parameters indicates that the states immediately above the Fermi level in $Cu_2S_2^-$ have a moderate copper contribution needed for hole delocalization in the plane of the layer.

The other copper−sulfur layers have similar electronic structures; we calculate that the holes in the valence band are delocalized over copper and sulfur atoms.

Relative Stabilities of the Copper−Sulfur Layers

There exist several representatives of the $MCu_{2n}S_{n+1}$ series, but their stabilities differ. $TlCu_2S_2$ is the only compound known for $n = 1$. Interestingly, when $TlCu_2S_2$ decomposes upon heating, $TlCu_4S_3$ is produced as one of the products.[2] The $Cu_4S_3^-$ layers are more stable—they form crystals with four different cations (Tl^+, K^+, Rb^+, and Cs^+). For $n = 3$, again only one compound has been found—$TlCu_6S_4$.

In order to address the relative stabilities of the layered compounds, we need to choose the appropriate structural models and define what we mean by "relative stability" in the context of these models. The ability of the $Cu_4S_3^-$ layers to bind with various monovalent cations indicates that these layers themselves are the backbone of the corresponding crystals. It is logical then to focus on the relative stabilities of the $Cu_{2n}S_{n+1}^-$ layers. There are only two choices for the geometry of the layers, as discussed previously: the model geometry (bulk Cu_2S-like) and that compressed in the *xy* plane to the experimentally observed value of the lattice parameter *a*.

(33) A referee commented that another atomic parameter set (S 3p H_{ii} = −11.601 eV, Cu 3d H_{ii} = −13.367 eV, other parameters also differ from the ones used in the current paper) yielded charges of about +0.5 on Cu and −1.0 on S in $TlCu_3S_2$ (ref 4).

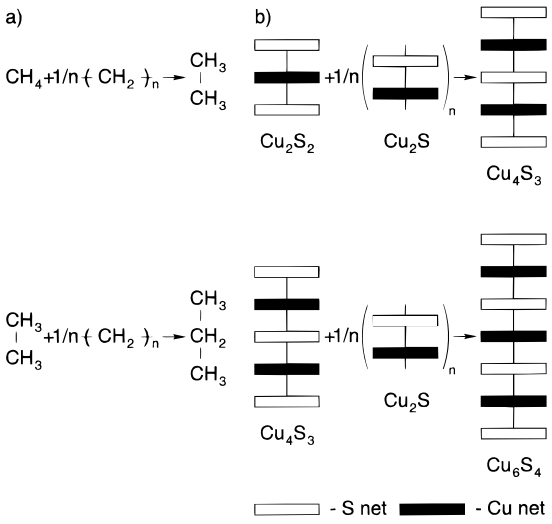

Figure 6. (a) Isodesmic reactions involving the first three alkane homologues and polyethylene. (b) Isodesmic reactions between copper−sulfur layers and copper sulfide.

Defining the relative stability is tricky because the stoichiometry of $Cu_{2n}S_{n+1}^-$ varies with *n*. We can utilize the interesting approach of so-called "isodesmic" reactions, developed in the field of *ab initio* calculations of organic molecules. A reaction is termed isodesmic if the number of bonds of a given type remains unchanged, but their relative positions change.[34] This definition can be illustrated with the following reaction:

$$CH_3CH_2CH_3 + CH_4 \rightarrow 2CH_3CH_3$$

There are 2 single C−C bonds and 12 C−H bonds on either side of this equation, but their relative positions differ (e.g. the two C−C bonds are in the same molecule on the left-hand side, but in separate molecules on the right-hand side). One may be interested in cases when the energy change in an isodesmic reaction is nearly zero, which indicates good transferability of bonds of the same type between different molecules, or in cases when the energy change deviates substantially from zero, due to changes in the character of the bonds. The phenomenon of aromaticity is a good example of the latter situation. We will address both scenarios.

Before the concept of isodesmic reactions is applied directly to the two-dimensional layers and three-dimensional copper sulfide, a simpler example needs to be studied. In anticipation of the task of relating structures of different dimensionalities, a case dealing with molecules and a one-dimensional polymer is considered (see Figure 6a). Two isodesmic reactions relate the first three alkane homologues. Any two successive homologues differ by a CH_2 group and a C−C single bond. A polyethylene chain, actually its chemical unit cell containing *exactly* one CH_2 group and one C−C single bond (the structural unit cell of transoid polyethylene has two CH_2 units), is used as a source of the CH_2 increment. The heats of these reactions (both calculated and measured experimentally) are small. This observation can be phrased in several different, but equivalent, ways: (a) C−C single bonds and C−H bonds in alkanes are transferable between different molecules; (b) the energy per one CH_2 unit is nearly independent of the size of the alkane molecule; (c) the energy of linear C_mH_{2m+2} molecules is a virtually linear function of *m*.

(34) Hehre, W. J.; Ditchfield, R.; Radom, L.; Pople, J. A. *J. Am. Chem. Soc.* **1970**, *92*, 4796.

Table 3. Changes in Electronic Energy for Isodesmic Reactions Involving Model Copper−Sulfur Layers

	ΔE ($q = -2$), eV	ΔE ($q = -1$), eV
$Cu_2S_2^q + Cu_2S \rightarrow Cu_4S_3^q$	−0.023	−0.320
$Cu_4S_3^q + Cu_2S \rightarrow Cu_6S_4^q$	−0.002	−0.159
$Cu_6S_4^q + Cu_2S \rightarrow Cu_8S_5^q$	0.000	−0.061

The case of the $Cu_{2n}S_{n+1}$ layers is conceptually similar. The corresponding isodesmic reactions are shown in Figure 6b. Now instead of a zero-dimensional building block (CH_2), a two-dimensional building block (a copper net and a sulfur net) is used. A potentially useful hypothesis, which will be tested shortly, can be stated: the bonding between a copper net and a sulfur net in the middle of a model Cu_4S_3 or a model Cu_6S_4 layer should be similar to that in bulk Cu_2S, due to the fact that the local geometries around the copper and sulfur atoms forming the bonds are the same in all three structures. This is analogous to the similarity between the C−C bonds in ethane, propane, and polyethylene. The same logic suggests that the bonding between the outermost sulfur net and the copper net closest to it should not change significantly in the $Cu_{2n}S_{n+1}$ series, parallel to the lack of change of the C−H bond character in terminal methyl groups of alkane molecules. Note that neither the reactions involving alkanes nor the reactions involving copper−sulfur layers are real; they are merely convenient mental constructions, which can be used to assess the relative stabilities of these compounds.

However, it is more than just the geometrical arrangement of atoms that determines the bonding in a system. Electron count is also essential; for instance, the presence of holes in the valence band of $Cu_{2n}S_{n+1}^-$ was shown to affect the Cu−S bonding. This again forces us to consider the corresponding closed shell system, $Cu_{2n}S_{n+1}^{2-}$, along with the more realistic $Cu_{2n}S_{n+1}^-$.

Now the changes in electronic energy for the reactions shown in Figure 6b can be calculated. Table 3 presents the results for both singly and doubly charged model layers; one more reaction, which involves a Cu_8S_5 layer from the as yet unsynthesized MCu_8S_5, is considered. Note that in the case of closed-shell layers, ΔE for the first reaction deviates only slightly from zero and the other two ΔEs are negligible. This is a manifestation of the fact that the Cu−S bonding in the middle of the $Cu_{2n}S_{n+1}^{2-}$ layers is like that in bulk copper sulfide (in the absence of holes). In other words, the energy of a $Cu_{2n}S_{n+1}^{2-}$ layer increases by a constant amount (the same as the energy of bulk copper sulfide per Cu_2S unit) when n is incremented by 1. The energy changes for the corresponding reactions involving singly charged copper−sulfur layers are substantially negative. The Cu−S bonding is no longer the same in the middle of $Cu_{2n}S_{n+1}^-$ layers, which have holes, and closed-shell Cu_2S.

Table 3 indicates that increasing the thickness of a singly charged copper−sulfur layer makes it more stable. A simple model explaining such behavior is shown in Figure 7. First, we can mentally separate the Cu_4S_3 layer shown into two kinds of regions on the basis of similarities in the local geometry around the Cu−S bonds. The inner region states, which we will refer to as simply bulk states, are bulk Cu_2S-like and thereby should have a similar dispersion in energy to that of the corresponding states in Cu_2S itself. The Cu_4S_3 states associated with the outermost sulfur nets and their bonding to the nearest copper net, which can be called surface states, should in turn resemble the corresponding states of the Cu_2S_2 layer. Then the total DOS for the Cu_4S_3 layer can be roughly approximated as a sum of the DOS for the Cu_2S_2 layer and bulk Cu_2S. The

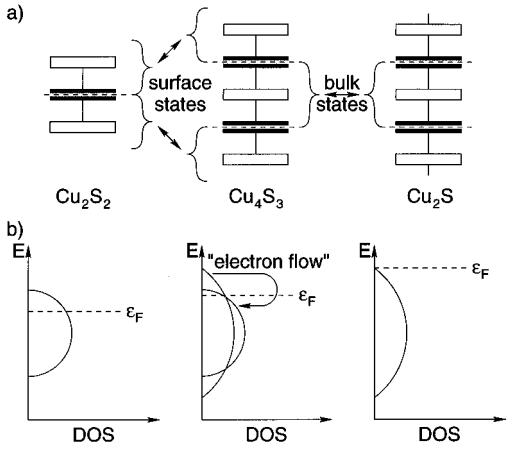

Figure 7. (a) Relationship between surface states in Cu_2S_2 and Cu_4S_3 and between bulk states in Cu_2S and Cu_4S_3. (b) Schematic DOS plots for the corresponding states in the valence band. The Fermi levels are shown for singly charged layers.

DOS plots for the valence bands (Cu d and S p bands) of the three systems are sketched in Figure 7. Note that the surface states are less dispersed in energy than the bulk states are. This behavior is typical, the consequence of the smaller number of nearest neighbors that surface atoms interact with.[30]

The source of the stabilization found in $Cu_4S_3^-$ with respect to $Cu_2S_2^-$ and Cu_2S lies in the electron transfer from the top of the valence band of Cu_2S to the lower-lying states immediately above the Fermi level in $Cu_2S_2^-$. Of course, one has to realize that this electron transfer can be discussed only in relation to our model. A similar explanation holds for each of the other two isodesmic reactions involving copper−sulfur layers.

More facts are needed to justify the use of this model. The most direct approach would be to compare the three DOS plots quantitatively to verify the additivity of densities of states assumed in the model. However, the k-point sets used to produce the corresponding DOS plots are incommensurate due to different dimensionalities of copper−sulfur layers and copper sulfide. The comparison of valence band widths (Cu d and S p bands combined) and the Fermi energies is a more justifiable alternative. The widest valence band is found in copper sulfide (5.87 eV) and the narrowest in $Cu_2S_2^-$ (4.38 eV), in accord with the model. However, the width of the valence band in $Cu_4S_3^-$ (5.17 eV) is less than that in Cu_2S. The order of the Fermi energies also agrees with the sketch in Figure 7: copper sulfide has the highest Fermi energy of the three structures (−11.39 eV) and $Cu_2S_2^-$ has the lowest (−12.05 eV). The Fermi level in $Cu_4S_3^-$ lies at −11.73 eV.

The model assumes no change in the density of surface states between Cu_2S_2 and Cu_4S_3 and no change in the density of bulk states between Cu_2S and Cu_4S_3. Therefore, if the valence bands are completely filled, no change in the electronic energy is expected for the corresponding isodesmic reaction. This fact also agrees with the data presented in Table 3.

Finally, the electron flow from the top of the valence band of the bulk states to the surface states (also shown in Figure 7) actually results in more negative computed charges on the outer sulfur net in $Cu_4S_3^-$ (−0.83) as compared to that in $Cu_2S_2^-$ (−0.71), as one would expect. At the same time, the charge on the middle sulfur net in $Cu_4S_3^-$ (0.01) is more positive than the charge on sulfur in bulk copper sulfide (−0.20).

We believe that we demonstrated that, to a good approximation, the model presented in Figure 7 is valid. It suggests that the $Cu_2S_2^-$ is the least stable layer in the series, each layer being more stable than the previous one. This result, however, is valid only when the geometry of the copper−sulfur layers is assumed

to be as in the model (bulk Cu_2S-like). But the energy of a layer also depends on the lattice parameter *a*, as was shown previously. It was computed that the energy of each layer decreases when *a* is varied from the model value of 3.94 Å to the experimentally observed value. The energy change for the first two isodesmic reactions shown in Table 3 can be computed using the compressed-layer energies. We calculate the energy changes for the two reactions to be −0.297 and 0.076 eV, respectively. This finding implies that the $Cu_4S_3^-$ layer is the most stable one in the series, the $Cu_2S_2^-$ still remaining the least stable. This stability order agrees pleasingly with the facts known: $TlCu_2S_2$ yields $TlCu_4S_3$ when heated, MCu_4S_3 exists for a variety of M, and MCu_6S_4 is found to exist only with M = Tl. However, this result should be taken with caution, because now the local geometry of the bulk and surface regions *changes* in the isodesmic reactions (while the copper−sulfur layers are taken to be in the compressed forms, the Cu_2S geometry is left ideal). Such a change introduces a new variable into the already approximate model.

Still, a useful conclusion can be stated; either version of the above discussed model, the one using idealized geometries or the one using experimental values of *a*, computes the $Cu_4S_3^-$ layer to be approximately 0.3 eV per unit cell more stable than Cu_2S and $Cu_2S_2^-$.

Conclusions

The most important feature of the $Cu_{2n}S_{n+1}^-$ layers is the presence of one hole per unit cell. The states at the top of the valence band, which host the hole, were found to be Cu−S and Cu−Cu antibonding; this was shown to be the reason for the observed contraction in the plane of the layers. High hole conductivity in $MCu_{2n}S_{n+1}$ was connected to the substantial delocalization of these states in the plane of the copper−sulfur layers.

The relative stability of the layers was defined on the basis of the notion of isodesmic reactions. The $Cu_2S_2^-$ layer was found to be approximately 0.3 eV per unit cell less stable than $Cu_4S_3^-$.

Acknowledgment. Thanks are due to Gregory Landrum for extensive help with using his program as well as to Hugh Genin, Erika Merschrod, and Norman Goldberg for constructive criticism on the manuscript. The authors thank Rolf Berger and the referees for their comments. This work was supported by the National Science Foundation through research Grant CHE 94-08455. G.V. would also like to thank the Olin Foundation for support through a graduate fellowship.

Appendix

The following orbital exponents (ζ) and valence shell ionization potentials (H_{ii} in eV) were used in all calculations:[35] S 3s ζ 2.122, H_{ii} −20.0; S 3p ζ 1.827, H_{ii} −14.0; Cu 4s ζ 2.2, H_{ii} −11.4; Cu 4p ζ 2.2, H_{ii} −6.06; Cu 3d H_{ii} −14.0. Cu 3d orbitals were represented by sums of two exponents: $\zeta_1 = 5.95$ with the weighting coefficient $c_1 = 0.5933$ and $\zeta_2 = 2.30$ with $c_2 = 0.5744$. S 3p H_{ii} was optimized to −14.0 eV in order to reproduce the expected charge distribution in Cu_2S. A modified Wolfsberg−Helmholtz (weighted H_{ij}) formula[36] was employed.

An 84 *k*-point set was used in average properties calculations on bulk copper sulfide. The properties of the $Cu_{2n}S_{n+1}^{2-}$ layers were computed with a 120 *k*-point set. The open shell $Cu_{2n}S_{n+1}^-$ systems required a thorough sampling of the Fermi surface; a larger 325 *k*-point set was employed. The *k*-point sets were generated according to the algorithms of Ramirez and Böhm for two-[37] and three-dimensional[38] crystals.

IC951046+

(35) *Tables of Parameters for Extended Hückel Calculations*; collected by Alvarez, S., Universitat de Barselona, 1993.
(36) Ammeter, J. H.; Bürgi, H.-B.; Thibeault, J. C.; Hoffmann, R. *J. Am. Chem. Soc.* **1978**, *100*, 3686.
(37) Ramirez, R.; Böhm, M. C. *Int. J. Quantum Chem.* **1986**, *30*, 391.
(38) Ramirez, R.; Böhm, M. C. *Int. J. Quantum Chem.* **1988**, *34*, 571.